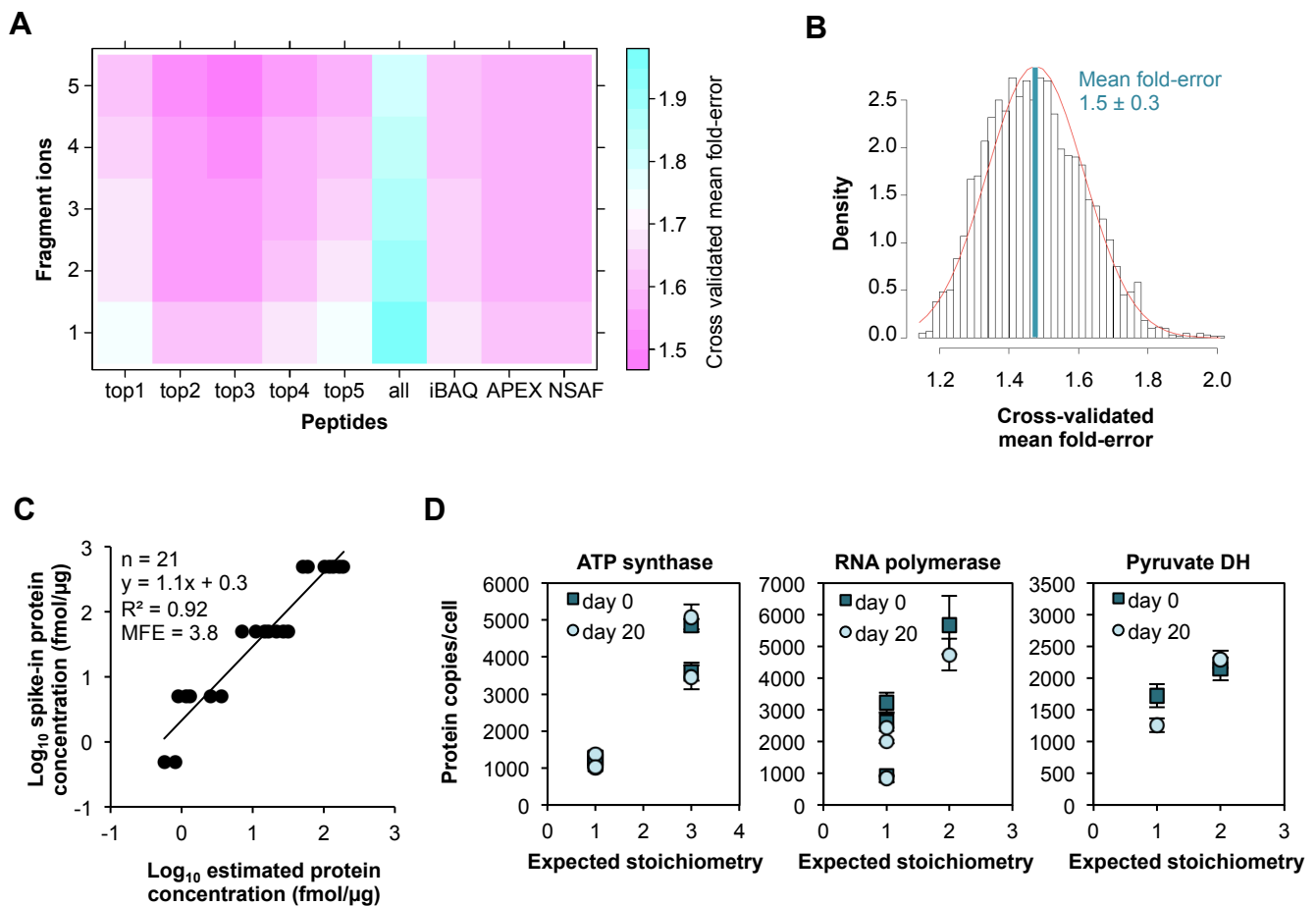


**Figure S1. SWATH MS data quality, linked to Figure 2.**

**(A)** Fraction of directly quantified peptide features by integration of a confidently assigned fragment ion peak group for at least one peptide (mScore represents the feature FDR and indicates the peak quality, the lower the better). Background extraction means that for these proteins no peptide could be confidently identified (mScore > 0.05) and therefore the protein intensity was obtained by integrating the background signal at the expected peptide retention time, generating a value that represents the maximally possible signal intensity for that peptide.

**(B)** Same as for (A), but on protein level. For every protein the best peptide feature over all runs (lowest average mScore) was selected as representative protein score.



**Figure S2. SWATH-based label-free absolute protein abundance estimation, linked to Figure 2.**

(A) Heatmap illustrating cross-validated mean fold errors for various published absolute label-free protein abundance estimation methods. The different methods were evaluated using the aLFQ R package (Rosenberger et al., 2014). All calculations were based on 30 endogenous anchor proteins, for which accurate absolute protein concentrations had been determined in all samples using stable isotope-labelled peptides. Remarkably, all absolute label-free methods resulted in a mean fold error  $< 2$ . The sum of the top 5 transitions of the top 3 peptides per protein had the lowest cross-validated mean fold error (1.5) and was selected for further analyses. (B) Cross-validated mean fold error distribution for the optimal model identified in (A). (C) A protein standard consisting of 48 human proteins at 6 different concentrations spanning 5 orders of magnitude (UPS2, Sigma-Aldrich) was spiked into two Mtb whole-cell lysates. For 21 out of the 48 human spike-in proteins, ranging from 0.5 to 500 fmol/ $\mu\text{g}$ , the criteria for absolute protein abundance estimation were fulfilled, i.e. at least 2 peptides per protein were quantified with high confidence. Linear correlation of the spike-in concentrations provided by the manufacturer and absolute protein abundance estimates using the top 5 transitions of the top 3 peptides per protein showed a high correlation coefficient ( $R^2 = 0.94$ ) and a mean fold error (MFE) of 3.8-fold. Hence, this analysis confirmed the validity of the absolute label-free abundance estimation approach on a completely independent set of proteins. (D) Absolute protein abundances determined in this study on a global cellular level reflected theoretical complex stoichiometries. The theoretical stoichiometry of subunits is indicated on the x-axis, while the estimated protein abundance is given on the y-axis. If the cell would produce exactly the amount of protein required to build the complex, the correlation would be perfect with a slope of 1 and a y-axis intercept of 0.

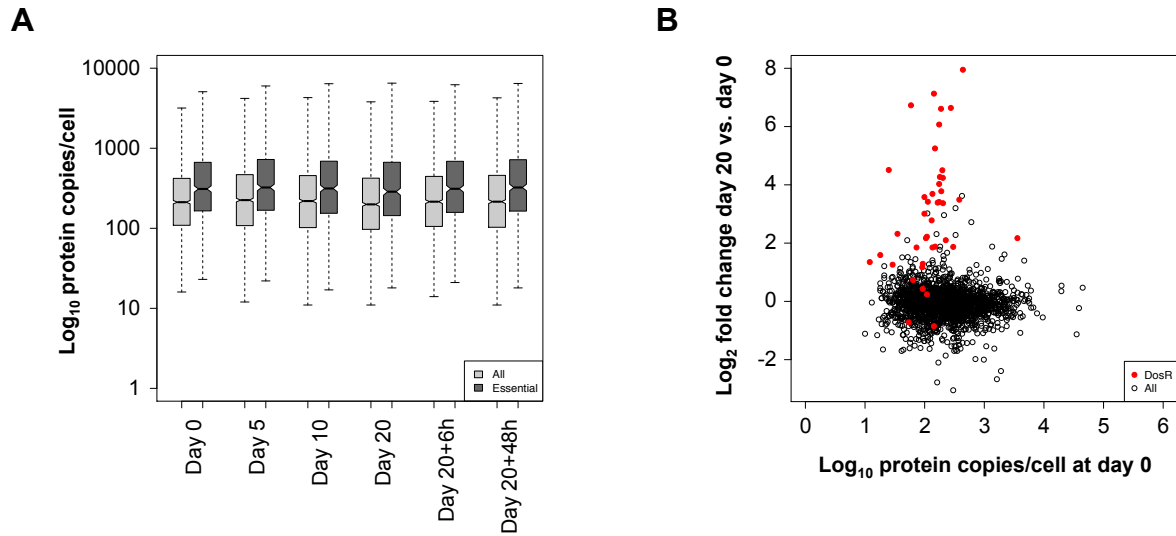


**Figure S3. Absolute protein abundances of essential genes and correlation between absolute and relative quantitative data, linked to Figure 3.**

**(A)** Protein products of essential genes for optimal growth in vitro (Griffin et al., 2011) (dark grey) were on average significantly more abundant compared to all other proteins (light grey) during the entire course of the experiment. A two-sample Kolmogorov-Smirnov test was applied to compare the essential protein set ( $n=606$ ) to all proteins ( $n=2023$ ) resulting in a  $p$ -value  $< 10^{-8}$  for all time points. **(B)** Comparison of absolute concentration (at day 0) and  $\log_2$  fold change of day 20 versus day 0 indicates that there is no clear correlation between absolute abundance and fold changes. Proteins highlighted in red are members of the DosR regulon.

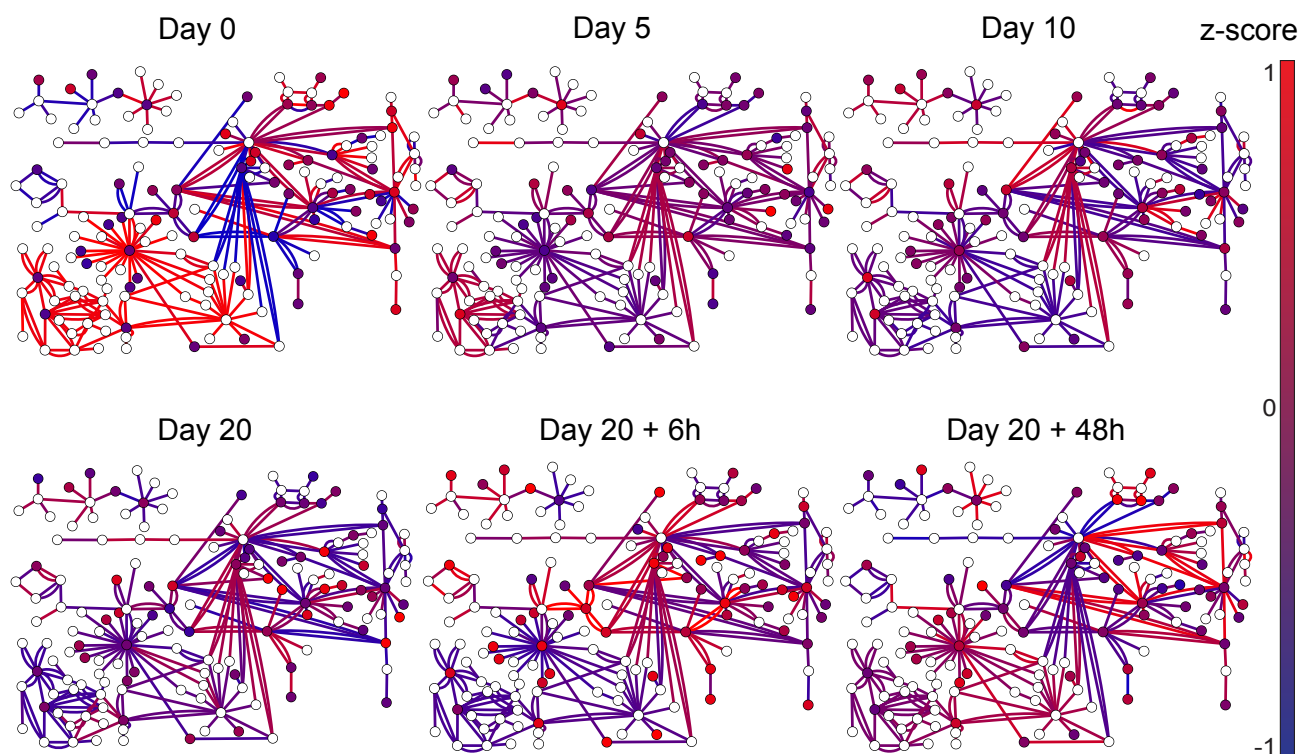


**Figure S4. Regulation of metabolic subnetworks, linked to Figure 6.**

Network representing connected reactions (path length  $\geq 4$ ), for which all corresponding enzymes were changed significantly in at least one time point (fold change  $\geq 1.5$ , p-value  $\leq 0.01$ ). Colouring represents protein abundances (edges) and metabolite intensities (nodes) normalised by z-score.

## Supplemental Figure Legends

### Figure S1. SWATH MS data quality, linked to Figure 2

**(A)** Fraction of directly quantified peptide features by integration of a confidently assigned fragment ion peak group for at least one peptide (mScore represents the feature FDR and indicates the peak quality, the lower the better). Background extraction means that for these proteins no peptide could be confidently identified (mScore > 0.05) and therefore the protein intensity was obtained by integrating the background signal at the expected peptide retention time, generating a value that represents the maximally possible signal intensity for that peptide. **(B)** Same as for (A), but on protein level. For every protein the best peptide feature over all runs (lowest average mScore) was selected as representative protein score.

### Figure S2. SWATH-based label-free absolute protein abundance estimation, linked to Figure 2

**(A)** Heatmap illustrating cross-validated mean fold errors for various published absolute label-free protein abundance estimation methods. The different methods were evaluated using the aLFQ R package (Rosenberger et al., 2014). All calculations were based on 30 endogenous anchor proteins, for which accurate absolute protein concentrations had been determined in all samples using stable isotope-labelled peptides. Remarkably, all absolute label-free methods resulted in a mean fold error < 2. The sum of the top 5 transitions of the top 3 peptides per protein had the lowest cross-validated mean fold error (1.5) and was selected for further analyses. **(B)** Cross-validated mean fold error distribution for the optimal model identified in (A). **(C)** A protein standard consisting of 48 human proteins at 6 different concentrations spanning 5 orders of magnitude (UPS2, Sigma-Aldrich) was spiked into two Mtb whole-cell lysates. For 21 out of the 48 human spike-in proteins, ranging from 0.5 to 500 fmol/μg, the criteria for absolute protein abundance estimation were fulfilled, i.e. at least 2 peptides per protein were quantified with high confidence. Linear correlation of the spike-in concentrations provided by the manufacturer and absolute protein abundance estimates using the top 5 transitions of the top 3 peptides per protein showed a high correlation coefficient ( $R^2 = 0.94$ ) and a mean fold error (MFE) of 3.8-fold. Hence, this analysis confirmed the validity of the absolute label-free abundance estimation approach on a completely independent set of

proteins. **(D)** Absolute protein abundances determined in this study on a global cellular level reflected theoretical stoichiometries of members of multi-protein complexes. The theoretical stoichiometry of subunits is indicated on the x-axis, while the estimated protein abundance is given on the y-axis. If the cell would produce exactly the amount of protein required to build the complex, the correlation would be perfect with a slope of 1 and a y-axis intercept of 0.

**Figure S3. Absolute protein abundances of essential genes and correlation between absolute and relative quantitative data, linked to Figure 3**

**(A)** Protein products of essential genes for optimal growth in vitro (Griffin et al., 2011) (dark grey) were on average significantly more abundant compared to all other proteins (light grey) during the entire course of the experiment. A two-sample Kolmogorov-Smirnov test was applied to compare the essential protein set (n=606) to all proteins (n=2023) resulting in a p-value  $< 10^{-8}$  for all time points. **(B)** Comparison of absolute concentration at day 0 and  $\log_2$  fold change of day 20 versus day 0 indicates that there is no clear correlation between absolute abundance and fold changes. Proteins highlighted in red are members of the DosR regulon.

**Figure S4. Regulation of metabolic subnetworks, linked to Figure 6**

Network representing connected reactions (path length  $\geq 4$ ), for which all corresponding enzymes were changed significantly in at least one time point (fold change  $\geq 1.5$ , p-value  $\leq 0.01$ ). Colouring represents protein abundances (edges) and metabolite intensities (nodes) normalised by z-score.

## Supplemental Table Legends

### **Table S1. Proteome-wide relative quantification by SWATH MS, linked to Figure 2**

Results of relative SWATH MS-based quantification of proteins in Mtb (sheet “Mtb relative”) and BCG (sheet “BCG relative”) compared to day 0 of the hypoxic time course. For Mtb, p-values were adjusted for multiple hypotheses testing using the Benjamini-Hochberg method. For BCG, no p-values were calculated because no biological replicates were available. For subsequent analyses, significantly changing proteins were considered if they had a fold change > 1.5 and a p-value < 0.01 in at least one of the conditions compared to day 0. For proteins with identical amino acid sequences (TubercuList v2.6 R27) only one representative protein was kept (see list in sheet “Description”).

### **Table S2. Anchor protein absolute quantification, linked to Figure 2**

To investigate the correlation between peptide concentration and SWATH signal intensity and to determine the lower limit of quantification for every stable isotope labelled standard peptide, a dilution series experiment spanning 30 to 0.1 fmol/μg in a constant background (1 μg Mtb whole cell lysate) was performed (sheet “Dilution series”). All peptides showed a good linear correlation as indicated by a Pearson  $R^2$  above 0.94, slopes close to 1 and axis intercepts close to 0. Furthermore, quantified endogenous peptide concentrations were not significantly lower than the lower limit of quantification determined by the dilution series experiment. Absolute peptide abundances for 51 peptides representing 30 anchor proteins are given in sheet “Absolute peptides”. Absolute protein abundances for 30 anchor proteins are given in sheet “Absolute proteins”. For those proteins for which two absolutely quantified peptides were available, individual peptide concentrations were averaged. Concentrations are given in fmol peptide per μg of total cell extract (fmol/μg).

Abbreviation: CAM = Carbamidomethylation

### **Table S3. Dynamic proteome-wide absolute abundance estimates, linked to Figure 2**

Results of label-free SWATH MS-based absolute protein abundance estimation of proteins in Mtb (sheet “Mtb absolute per sample”) and BCG (sheet “BCG absolute per sample”) in the hypoxic time course. Absolute protein abundances were estimated

based on the Top3 approach and linear regression of a set of accurately quantified anchor proteins. Cross-validation analysis indicated for the abundance estimates an average fold-error of approximately 2. Absolute concentrations are given in protein copies per cell, assuming a cellular protein concentration of 0.2 g/ml and a cell volume of  $0.5 \mu\text{m}^3$ . For Mtb, absolute protein abundances of biological replicates were averaged and standard deviations were calculated (sheet “Mtb absolute per condition”). Technical replicate (Rep3b) was not considered in this calculation. For BCG no biological replicates were available and absolute protein abundances represent the average over the two technical replicates (sheet “BCG absolute per condition”). For proteins with identical amino acid sequences (TubercuList v2.6 R27) only one representative protein was kept (see list in sheet “Description”).

#### **Table S4. Subnetwork analysis, linked to Figure 6**

Abbreviations of all metabolites contained in the subnetworks extracted from the genome-scale model are given in sheet “Metabolite abbreviations”. Metabolites which were not used in building the reaction-reaction connections for the subnetwork analysis are given in sheet “Metabolites excluded”. Z-scores of proteins which were part of the subnetwork of regulated reactions were calculated by subtracting from the mean fold change of the absolute abundance estimate over the biological replicates from one time point the mean fold change across all time points and dividing the result by the standard deviation across time points (sheet “Protein z-scores”). Protein pathway assignments were exported from the TBDB database.

#### **Table S5. Metabolite data, linked to Figure 6**

Raw ion intensities obtained by direct injection MS using a quadrupole-coupled time of flight mass spectrometer at low mass range settings (sheet “Raw intensities”). The genome scale metabolic model of Mtb was used to compile a metabolite reference list. Ions were assigned to metabolites using this list, allowing a mass tolerance of 1 mDa and applying an intensity cut-off of 1500 counts. For each metabolite only the best corresponding ion was kept. (For two metabolites, methanol and UDP-N-glycolylmuramoyl-L-alanyl-D-glutamate, two ions were matching equally well). For each sample, ion intensities were normalised by the mean ion intensity across all detected ions (sheet “Normalised intensities”). Normalised intensities were then standardised with z-scores and are given in sheet “Z-scores”. The z-score was calculated as follows:



$(\text{value} - \text{mean}(\text{values across conditions}))/\text{std}(\text{values across conditions})$ . Fold changes of averaged intensities (across four replicates) to time point day 0 are given in sheet “Fold changes and p-values”. P-values were obtained from a two-sample t-test with unequal variances (ttest2 function in Matlab) and adjusted for multiple hypotheses testing with the Benjamini-Hochberg method.

**Table S6. Enzyme turnover frequency coefficients, linked to Figure 7**

For each enzyme, EC number information was downloaded from the BRENDA database using an in-house written Python script. If available, the median value for the turnover frequency coefficient (kcat) reported for Mtb and the median value reported for all organisms was recorded. For estimation of maximum reaction velocities (Vmax), the median kcat for Mtb was used, if available. In case no Mtb-specific value was reported, the median kcat value of all organisms was used. If for a specific enzyme no kcat information was available at all, 1 was taken as default value. Mappings between protein Rv and enzyme EC numbers were obtained from the TBDB database. For PfkA and PfkB, turnover frequency values were calculated based on activity values obtained directly from the literature (Phong et al., 2013).

**Table S7. TBDB pathway enrichment in the set of significantly changing proteins, linked to Figure 7**

Results of pathway enrichment of all significantly up or down-regulated proteins. TBDB pathway definitions were downloaded from the TBDB database. In every sheet of the Excel file, three columns are provided for each time point: enrichment p-value, adjusted p-value (Benjamini-Hochberg), and enrichment statistics (number of pathway proteins in the subset, size of the protein subset, number of proteins in the pathway, total number of proteins). For all time points, time point day 0 was used as a reference. For time points day20+6h and day20+48h day 20 was also used as a reference. The overview table in the sheet “Description” describes in detail the information in the eight data sheets of this Excel file.

## Supplemental Experimental Procedures

### Reference proteome annotation

As a reference annotation of the Mtb proteome we used TubercuList v2.6 R27 (March 2013). The protein sequence FASTA file was downloaded from the web (<http://tuberculist.epfl.ch>). The first amino acid of each protein was replaced by a methionine and all internal stop codons and other non-amino acid characters were removed from the protein sequences. In Mtb several proteins encoded at different locations in the genome have identical sequences. These redundancies were removed by deleting multiple entries of the same protein sequence and just keeping the first one as a representative (CD-HIT tool: <http://cd-hit.org>). The number of annotated protein sequences in TubercuList v2.6 R27 is 4031. After removal of identical sequences, 3990 unique protein sequences remain. We based our analysis on the unique proteins only. A list of identical protein sequences and the corresponding base protein kept for this study is given in the “Description” tab of Table S1.

### Bacterial cultures

Mtb H37Rv (ATCC #27294) and *M. bovis* BCG was grown in Dubos broth enriched with Dubos Medium Albumin (Becton Dickinson) at 37°C. Hypoxia experiments were started by diluting exponentially growing bacteria ( $OD_{600}=0.4$ , day 0) to an  $OD_{600}$  of 0.005 as described earlier (Lim et al., 1999; Wayne and Hayes, 1996). The tightly sealed glass vials with a fixed headspace-culture ratio of 1:2 were kept closed until harvesting to prevent exposure to external oxygen. Samples were taken at 5, 10 and 20 days of the hypoxic time course (day 5, day 10 and day 20). After sampling at day 20, remaining glass vials were opened and cultures were transferred into new vessels for aerated incubation at 80 rpm and 37°C. Further time points were sampled from the re-aerated cultures after 6 and 48 hours (day 20+6h and day 20+48h).

### Proteomics sample preparation

Bacteria from 5 Wayne flasks (87.5 ml) were harvested by centrifugation at 3000 g for 10 min and washed with ice-cold phosphate-buffered saline. Pellets were then resuspended in lysis buffer containing 8 M urea and 0.1% RapiGest, (#186001861, Waters) in 0.1 M ammonium bicarbonate buffer. The cell suspension was thoroughly vortexed and incubated at room temperature for 10 min while shaking at 1000 rpm. Subsequently,

bacilli were subjected to three 10-min cycles of sonication at 4°C (100% output, 50% intervals, Branson Sonifier 450, Emerson) and additionally disrupted by three 10-min cycles of bead beating at 4°C using glass beads with a diameter of 0.5 mm (SIGMA #G8772). After each cycle, lysates were centrifuged for 10 min at 16,000 g and fresh lysis buffer was added. In total, 250 µl of lysis buffer was added. Protein lysates were sterile filtered twice for decontamination and protein concentration was determined using a bicinchoninic acid (BCA) assay according to the manufacturer's protocol (#23227, Thermo Fisher Scientific). From each sample only 50 µg of protein was used for subsequent steps.

The Universal Proteomics Standard 2 (UPS2, Sigma-Aldrich) is a set of 48 unlabelled human proteins at 6 different concentrations (8 proteins per concentration) spanning 5 orders of magnitude (50 pmol to 500 amol, 10.6 µg total protein). One tube was dissolved in 40 µl of lysis buffer. 20 µl of this UPS solution added to one replicate of the samples from day 0 and day 20, whereas to all other samples, 20 µl of lysis buffer was added.

Protein disulfide bonds were reduced by adding 5 mM tris(2-carboxyethyl)phosphine (TCEP) and incubating for 30 min at 30°C. Next, the free cysteine residues were alkylated by adding 40 mM iodoacetamide and incubating for 60 min in the dark at room temperature. Subsequently, the samples were diluted with 0.05 M ammonium bicarbonate buffer to reach a urea concentration of 6.7 M. 0.5 µg LysC (#125-05061, Wako) was added to each sample (w/w 1:100) and incubated at 30°C for 6 hours. Then the samples were further diluted to a urea concentration <2 M and 1 µg of sequencing-grade modified trypsin (#608-274-4330, Promega) was added (w/w 1:50). The samples were incubated over night at 30°C with gentle shaking at 300 rpm. At this step 51 isotopically labelled synthetic reference peptides (AQUA QuantPro, Thermo Fisher Scientific) for absolute quantification of the 30 anchor proteins were added to the samples in concentrations roughly adjusted to the corresponding endogenous peptides. To stop the tryptic digest and to precipitate RapiGest the pH was lowered to 2 using trifluoro acetic acid (final concentration of ~1%) followed by an incubation for 30 min at 37°C with shaking at 500 rpm. The water-immiscible degradation product of RapiGest was pelleted by centrifugation at 16,000 g for 10 min.

The cleared peptide solution was desalted with C18 MicroSpin columns (The Nest Group, 5-60 µg loading capacity). Prior to use, the C18 columns were activated with 100% methanol, followed by 80% acetonitrile (ACN)/0.1% TFA, followed by equilibration

with 2% ACN/0.1% TFA. After loading the sample, the columns were washed with 2% ACN/0.1% TFA. Finally, peptides were eluted with 40% ACN/0.1% TFA, dried under vacuum, and resolubilised in 46  $\mu$ l 2% ACN/0.1% FA and 4  $\mu$ l iRT peptide mix (RT-kit WR, Biognosys) to a final concentration of 1 mg/ml. The iRT peptides are important to allow determination of system-independent retention times (iRT) for each peptide relative to these calibration peptides as recently described by Escher and colleagues (Escher et al., 2012).

### **SWATH assay library generation**

As an input for the SWATH assay library the following samples were acquired on a TripleTOF 5600 in data/information-dependent acquisition (IDA) mode: (i) 19 pools of up to 1000 crude synthetic peptides (Schubert et al., 2013) each, (ii) 24 off-gel electrophoresis (OGE) fractions of an Mtb lysate consisting of bacteria from exponential and stationary phase cultures (Schubert et al., 2013), (iii) 12 unfractionated whole cell lysates of Mtb and *M. bovis* BCG during hypoxic stress. To each of the 55 samples iRT peptides (RT-kit WR, Biognosys) were added.

The TripleTOF 5600 mass spectrometer (AB Sciex) was coupled to a nanoLC 1Dplus system (Eksigent) and the chromatographic separation of the peptides was performed on a 20-cm emitter (75  $\mu$ m inner diameter, #PF360-75-10-N-5, New Objective) packed in-house with C18 resin (Magic C18 AQ 3  $\mu$ m diameter, 200 Å pore size, Michrom BioResources). A linear gradient from 2-35% solvent B (98% ACN/0.1% FA) was run over 90 min (synthetic peptide pools) or 120 min (OGE fractions and whole cell lysates) at a flow rate of 300 nl/min. The mass spectrometer was operated in IDA mode with a 500 ms survey scan from which up to 20 ions exceeding 250 counts per second were isolated with a quadrupole resolution of 0.7 Da, using an exclusion window of 20 s. Rolling collision energy was used for fragmentation and an MS2 spectrum was recorded after an accumulation time of 150 ms.

Raw data files (wiff) were centroided and converted into mzML format using the AB Sciex converter (beta version 2011) and subsequently converted into mzXML using openMS (version 1.8). The converted data files were searched using the search engines X!Tandem (k-score, version 2013.06.15.1), Omssa (version 2.1.9), Myrimatch (version 2.1.138), and Comet (version 2013.02, revision 2) against the 3990 annotated Mtb protein sequences (TubercuList, see above), ~100 common contaminants, the 48 UPS proteins and the sequences of the iRT peptides. Further, for every of these target

proteins a corresponding decoy protein was generated based on concatenated pseudo-reversed peptide sequences (the sequence of every tryptic peptide is reversed while keeping lysine and arginine residues at the C-terminus). Only fully tryptic peptides with up to two missed cleavages were allowed for the database search. The tolerated mass errors were 50 ppm on MS1 level and 0.05 Da on MS2 level. Carbamidomethylation of cysteines was defined as a fixed modification and methionine oxidation as a variable modification. The search results were processed with PeptideProphet (Keller et al., 2002) and iProphet (Shteynberg et al., 2011) as part of the TPP 4.7.0 (Deutsch et al., 2010). To determine the iProphet cut-off corresponding to a 1% protein FDR, the software tool MAYU (version 1.0.7) (Reiter et al., 2009) was applied. The SWATH assay library was constructed from the iProphet results with an iProphet cut-off of 0.990315, corresponding to a 1% FDR on protein level. The raw and consensus spectral libraries were built with SpectraST (version 5.0) (Lam et al., 2007; 2008) using the `-cICID_QTOF` option for high resolution and high mass accuracy and `-c_IRT` and `-c_IRR` options to normalise all retention times according to the iRT peptides with a linear regression. The 5 most intense y and b fragment ions of charge state 1 and 2 were extracted from the consensus spectral library using `spectrast2tsv.py` from `msproteomicstools` (<https://pypi.python.org/pypi/msproteomicstools>). Fragment ions falling into the swath window of the precursor were excluded as the resulting signals are often highly interfered. All miscleaved and methionine oxidised peptides were removed before converting the library into TraML format using the OpenMS tool `ConvertTSVToTraML` (version 1.10.0). Decoy transition groups were generated based on shuffled sequences (decoys similar to targets were excluded) by the OpenMS tool `OpenSwathDecoyGenerator` (version 1.10.0) and appended to the final SWATH library in TraML format.

### **SWATH data acquisition**

The TripleTOF 5600 mass spectrometer was set up as described above, but operated in SWATH mode (Gillet et al., 2012) using the following parameters: For the liquid chromatography a linear gradient from 2-35% solvent B (98% ACN/0.1% FA) was run over 120 min at a flow rate of 300 nL/min. Acquisition of a 100-ms survey scan was followed by acquisition of 32 fragment ion spectra from 32 precursor isolation windows (swaths) of 26 m/z each. The swaths were overlapping by 1 m/z and thus cover a range of 400-1200 m/z. The SWATH MS2 spectra were recorded with an accumulation time of

100 ms and cover 100-2000 m/z. The collision energy for each window was determined according to the calculation for a charge 2+ ion centred upon the window with a spread of 15. Raw data files (wiff) were converted into mzXML format using ProteoWizard (version 3.0.3316) (Chambers et al., 2012).

### **SWATH data analysis with OpenSWATH**

The SWATH data was analysed using OpenSWATH (Röst et al., 2014) with the following parameters: Chromatograms were extracted with 50 ppm around the expected mass of the fragment ions and with an extraction window of +/-5 min around the expected retention time after iRT alignment. The best model to separate true from false positives (per run) was determined by pyprophet with 10 cross-validation runs (Teleman et al., 2014). The runs were subsequently aligned with a target FDR of 0.01 (mScore < 0.00159) and a maximal FDR of 0.05 for aligned features (Röst et al., unpublished). In the absence of a confidently identified feature, the peptide and protein intensities were obtained by integration of the respective background signal at the expected peptide retention time (Röst et al., unpublished).

### **Refinement of the SWATH dataset**

To reduce the size of the output data and remove low-quality features, a filtering step was introduced to only keep the 10 most intense peptides per protein and only features that were identified with an FDR of < 0.01 in all replicates of at least one condition, i.e. time point. Further, the 21 most abundant proteins in the 24 Mtb samples were manually requantified using Skyline (MacLean et al., 2010), because OpenSWATH could not consistently integrate the distorted peak shapes resulting from overloaded chromatography. The requantified peaks can be visualised in Panorama: [panoramaweb.org/labkey/Mtb\\_requant.url](http://panoramaweb.org/labkey/Mtb_requant.url).

### **Relative protein quantification**

To obtain fold changes and corresponding p-values of all proteins compared to day 0 (exponential growth), the software MSstats (version MSstats.daily 2.3.5) was used (Choi et al., 2014). The input data was reduced to maximally 5 peptides per protein and normalised such that the median of each sample was constant. The fold changes and p-values of all time points compared to day 0 were obtained by linear mixed models with expanded scope of biological and technical replication. P-values were adjusted for

multiple hypotheses testing using the Benjamini-Hochberg method as implemented in MSstats. For subsequent analysis, significantly changing proteins were considered if they had a fold change > 1.5 and a multiple hypotheses testing-adjusted p-value < 0.01 in at least one of the time points compared to day 0. K-means clustering was performed using Pearson correlation (MultipleExperiment Viewer v4.8.1). For cluster analysis, the data was standardised by subtracting the mean and dividing by the standard deviation.

### **Absolute label-free protein abundance estimations**

For absolute label-free abundance estimations of all proteins identified by SWATH MS, 30 anchor proteins were selected covering a wide abundance range of the Mtb proteome (Schubert et al., 2013). For each anchor protein one or two synthetic isotope-labelled reference peptides in defined concentrations as determined by amino acid analysis were spiked into the samples for accurate absolute quantification of these anchor proteins (see sample preparation paragraph). To ensure accurate absolute quantitation results, the linear dynamic quantification range and the lower limit of quantification for each reference peptide was determined by performing a dilution series experiment. In the end, 51 peptides showed good linear response (slope close to 1, axis intercept close to 0,  $R^2 > 0.94$ ) and suitable lower limit of quantification with respect to endogenous protein levels. All results of this experiment are summarised in Table S2 and can be visualised in Panorama: [panoramaweb.org/labkey/Mtb\\_dilutions.url](http://panoramaweb.org/labkey/Mtb_dilutions.url). Absolute concentrations of all anchor proteins over all samples were analysed manually using Skyline (MacLean et al., 2010) and corresponding raw chromatographic data are available in Table S2 and in Panorama: [panoramaweb.org/labkey/Mtb\\_anchors.url](http://panoramaweb.org/labkey/Mtb_anchors.url). Integrated peak areas of the reference and endogenous peptides were summed and from the obtained ratios the endogenous peptide concentration was determined in fmol/ $\mu$ g. Of note, in the here described absolute quantification procedure, which is based on monoisotopic peak areas measured with high-resolution mass spectrometry, we did not account for differences in the theoretical isotopic distributions between the light and heavy peptide forms.

The optimal model to combine SWATH MS intensities to a single protein MS signal was determined by Monte Carlo cross-validation (Ludwig et al., 2012) using the aLFQ R package (version 1.3.1) (Rosenberger et al., 2014). Summarising the five most intense transitions of the three most intense peptides per protein was the resulting model with the highest accuracy and was used to estimate proteome-wide concentrations from the SWATH MS signal intensities. For proteins detected with only two peptides absolute



abundance estimation was based on those two peptides, while proteins with only a single quantified peptide were excluded from further analysis.

### **Estimating protein copies per cell**

The raw unit of protein concentrations in the present study was in “fmol per  $\mu\text{g}$  of extracted protein” because this is the direct readout of our measurements and the most accurate way to present the data. However, for various applications it is desirable to work in the unit “protein copies per cell”. To convert “fmol per  $\mu\text{g}$  of extracted protein” into “protein copies per cell” two assumptions are required: (i) 100% of all proteins were extracted during sample preparation and (ii) the protein concentration of a cell is in the range of  $2 \times 10^6$  proteins/ $\mu\text{m}^3$ , which in the case of Mtb corresponds to  $\sim 1 \times 10^6$  proteins/cell (assuming a cell volume of  $0.5 \mu\text{m}^3$ ) (Milo, 2013). This value corresponds to a protein density of 0.2 g/ml, which was reported by Milo and colleagues (Milo, 2013) as a reasonable value for various cell types, including mammalian cells, budding yeast and *E. coli*. As an alternative to these assumptions, cells could be counted prior to lysis. While this is the standard approach for other organisms, such as yeast, in Mtb cell counting is challenging and can be highly error prone because the cells tend to form clumps which impede accurate microscopy-supported counting or counting of colony-forming units. When working in the unit of “copies per cell”, also potential changes in cell volume or cell wall enlargements - both have been described for Mtb in the Wayne model - might need to be taken into consideration (Cunningham and Spreadbury, 1998; Velayati et al., 2011; Wayne and Hayes, 1996). In the current work we assumed a constant cell size and protein density for bacilli grown exponentially and cells in hypoxia. Generally, it is important to note that absolute quantification by mass spectrometry-based proteomics can show a bias against membrane-associated proteins which might be less efficiently extracted during the sample preparation procedure.

### **Metabolic profiling**

To determine intracellular ATP levels, the biomass of 10 ml culture volume was sampled by the fast filtration protocol previously reported (Watanabe et al., 2011). Bacteria were decontaminated and metabolites were extracted in chloroform:methanol (2:1) at  $-80^\circ\text{C}$  over night. Samples were dried under nitrogen stream, resuspended in 100  $\mu\text{l}$  water and 10  $\mu\text{l}$  were analysed for the quantification of ATP by ultrahigh pressure liquid chromatography coupled to a triple quadrupole tandem mass spectrometer as previously



described (Buescher et al., 2010). ATP amounts were normalised to the colony-forming unit determined for each sample. Two independent Wayne cultures were analysed for each time point.

Untargeted measurements of metabolites was performed by direct injection mass spectrometry using a quadrupole-coupled time of flight instrument (Agilent 6550) at low mass-range settings following the published protocol (Fuhrer et al., 2011). The genome scale metabolic model of Mtb was used to compile a metabolite reference list. Ions were assigned to metabolites using this list and allowing a mass tolerance of 1 mDa and an intensity cut-off of 1500 counts as previously described (Fuhrer et al., 2011). For each ion, only the metabolite(s) with the highest annotation score was kept, and for each metabolite, only one ion with the highest annotation score was kept. The untargeted metabolic data was not normalised after data acquisition, but by collecting equal amounts of biomass for all samples (sample volume adjusted to the measured OD<sub>600</sub>).

### **Subnetwork analysis**

Basis for the subnetwork analysis was a genome-scale metabolic model of Mtb. Only reactions of which at least one enzyme was changing significantly (fold change  $\geq 1.5$ , p-value  $\leq 0.01$ ) were considered. Two reactions that share a metabolite were considered as connected. H<sub>2</sub>O, CO<sub>2</sub> and common cofactors were not considered as connecting metabolites (Table S4). Shortest path search (Yen, 1971) was performed between each two reactions in the resulting reaction-reaction network using the Matlab script kShortestPath (<http://www.mathworks.com/matlabcentral/fileexchange/32513-k-shortest-path-yen-s-algorithm>) and those with length  $\geq 4$  were visualised in Cytoscape. Network edges were coloured according to protein abundances (x) normalised to the mean values across conditions with the Matlab z-score function ( $z\text{-score}=(x-\text{mean}(x))/\text{std}(x)$ ). Subnetworks were assigned to metabolic classes according to TBDB annotations (<http://www.tbdb.org>) and manually grouped according to their temporal profiles. The genome scale model was further used to assign metabolites involved in each reaction to the corresponding enzymes. Pearson correlation coefficients were calculated for the z-scores of metabolites and corresponding enzymes for time profiles with time shifts +/-1 to capture delayed dependencies.

### **Maximal enzymatic reaction velocity estimation**

Maximal enzymatic reaction velocities ( $V_{max}$ ) were estimated per definition as absolute protein quantity multiplied by the enzyme turnover frequency (kcat). Turnover frequency coefficients were downloaded from the Brenda enzyme database (<http://www.brenda-enzymes.org>). Median values of all reported kcats (or only those reported for Mtb, if available) were taken (Table S6). If no kcat was available, 1 was set as default value. For the PfkA and PfkB isoenzymes the kcat was calculated based on the activity values (PfkA = 25.0 [nmol min<sup>-1</sup> purified protein mg<sup>-1</sup>], PfkB = 1.7 [nmol min<sup>-1</sup> purified protein mg<sup>-1</sup>]) (Phong et al., 2013) and enzyme molar masses (PfkA = 36879.99 [g mol<sup>-1</sup>], PfkB = 35401.37 [g mol<sup>-1</sup>]) as activity multiplied by molar mass (PfkA = 0.015 sec<sup>-1</sup>, PfkB = 0.001 sec<sup>-1</sup>).

### **Statistical analysis and gene set enrichment**

Metabolic pathway definitions were downloaded from the TB database TBDB (<http://www.tbdb.org>). Pathway enrichment was performed for protein set consisting of proteins passing the cutoff of absolute fold change  $\geq 1.5$ , adjusted p-value  $\leq 0.01$ . P-values were adjusted for multiple hypotheses testing with the Benjamini-Hochberg procedure. Gene set enrichment analysis method was adapted from Subramanian et al. for proteins and implemented in a Matlab script (Subramanian et al., 2005). A hypergeometric test was applied for each subset of size 1 to N (N is the size of the changing protein set) from the changing protein set, sorted by one of the following characteristics: fold change, absolute change and  $V_{max}$  change. For each pathway the lowest adjusted p-value from tests of different sizes was taken. For time points day 20+6h and day 20+48h day 20 was taken as a reference.

## Supplemental References

Chambers, M.C., MacLean, B., Burke, R., Amodei, D., Ruderman, D.L., Neumann, S., Gatto, L., Fischer, B., Pratt, B., Egertson, J., et al. (2012). A cross-platform toolkit for mass spectrometry and proteomics. *Nature Biotechnology* 30, 918–920.

Cunningham, A.F., and Spreadbury, C.L. (1998). Mycobacterial stationary phase induced by low oxygen tension: cell wall thickening and localization of the 16-kilodalton alpha-crystallin homolog. *J Bacteriol* 180, 801–808.

Deutsch, E.W., Mendoza, L., Shteynberg, D., Farrah, T., Lam, H., Tasman, N., Sun, Z., Nilsson, E., Pratt, B., Prazen, B., et al. (2010). A guided tour of the Trans-Proteomic Pipeline. *Proteomics* 10, 1150–1159.

Keller, A., Nesvizhskii, A.I., Kolker, E., and Aebersold, R. (2002). Empirical statistical model to estimate the accuracy of peptide identifications made by MS/MS and database search. *Anal Chem* 74, 5383–5392.

Lam, H., Deutsch, E.W., Eddes, J.S., Eng, J.K., King, N., Stein, S.E., and Aebersold, R. (2007). Development and validation of a spectral library searching method for peptide identification from MS/MS. *Proteomics* 7, 655–667.

Lam, H., Deutsch, E.W., Eddes, J.S., Eng, J.K., Stein, S.E., and Aebersold, R. (2008). Building consensus spectral libraries for peptide identification in proteomics. *Nature Methods* 5, 873–875.

Lim, A., Eleuterio, M., Hutter, B., Murugasu-Oei, B., and Dick, T. (1999). Oxygen depletion-induced dormancy in *Mycobacterium bovis* BCG. *J Bacteriol* 181, 2252–2256.

Reiter, L., Claassen, M., Schrimpf, S.P., Jovanovic, M., Schmidt, A., Buhmann, J.M., Hengartner, M.O., and Aebersold, R. (2009). Protein identification false discovery rates for very large proteomics data sets generated by tandem mass spectrometry. *Mol Cell Proteomics* 8, 2405–2417.

Shteynberg, D., Deutsch, E.W., Lam, H., Eng, J.K., Sun, Z., Tasman, N., Mendoza, L., Moritz, R.L., Aebersold, R., and Nesvizhskii, A.I. (2011). iProphet: multi-level integrative analysis of shotgun proteomic data improves peptide and protein identification rates and error estimates. *Mol Cell Proteomics* 10, M111.007690.

Teleman, J., Röst, H.L., Rosenberger, G., Schmitt, U., Malmström, L., Malmström, J.A., and Levander, F. (2014). DIANA-algorithmic improvements for analysis of data-independent acquisition MS data. *Bioinformatics* (Oxford, England).

Velayati, A.A., Farnia, P., Masjedi, M.R., Zhavnerko, G.K., Merza, M.A., Ghanavi, J., Tabarsi, P., Farnia, P., Poleschuyk, N.N., and Ignatyev, G. (2011). Sequential adaptation in latent tuberculosis bacilli: observation by atomic force microscopy (AFM). *Int J Clin Exp Med* 4, 193–199.